View Article Online / Journal Homepage / Table of Contents for this issue
Dynamic Article Links

Soft Matter

Cite this: *Soft Matter*, 2011, **7**, 9027

www.rsc.org/softmatter

PAPER

Membrane fusion of pH-sensitive liposomes – a quantitative study using giant unilamellar vesicles†

Sofie Trier, Jonas R. Henriksen and Thomas L. Andresen*

Received 4th May 2011, Accepted 21st June 2011
DOI: 10.1039/c1sm05818e

Published on 11 August 2011. Downloaded by Pennsylvania State University on 05/03/2016 05:08:12.

Drug delivery systems based on liposome carriers that are designed for induction of membrane fusion in response to the microenvironment have been investigated for more than two decades. However, most studies have focused on self-fusion among large unilamellar vesicles (LUVs) in solution, a system with limited biological relevance which suffers from averaging effects and non-trivial interpretation of results. Here we present a fusion assay capable of visualizing and quantifying heterogeneous fusion between fusogenic liposomes and stable giant unilamellar vesicles (GUVs), suitable for studying both lipid and content mixing. Fusion was visualized and quantified using fluorescence microscopy and a FRET-based lipid mixing assay and the number of fusion events with single GUVs was estimated. Fusogenic pH-sensitive oleic acid (OA):DOPE liposomes were used as a model system and fusion was quantified with giant vesicles containing 5 or 10 mol% positively charged lipids. It was shown that the number of fusion events with single GUVs after 30 min at room temperature is approximately 100 or 200 per 100 μm^2 of GUV surface, for 5 or 10 mol%, respectively. Furthermore, the mixing of the aqueous content during fusion was visualized and quantified, which showed that the content of the fusogenic liposomes is transferred essentially without leakage. Fusion was confirmed to be pH-dependent and is enhanced by electrostatic attraction between the fusing vesicles, which was demonstrated by the absence of fusion in experiments performed with negatively charged GUVs.

Introduction

Fusogenic pH-sensitive liposomes have received considerable attention due to their potential as drug delivery systems.[1–3] The fusogenic liposomes become unstable in response to changes in pH, *e.g.* in the endosomes of cancer cells after receptor mediated internalization,[4] and are able to fuse with target membranes under the right conditions. Thus, fusogenic liposomes are, theoretically, able to transfer both lipid-soluble and water-soluble compounds to a target cell.

pH-sensitive liposomes typically contain dioleoylphosphatidylethanolamine (DOPE), a lipid that adopts the non-bilayer inverted hexagonal phase, and a mildly acidic lipid such as oleic acid.[3,5] The mixture forms vesicles at pH levels above the pK_a of oleic acid, due to the large effective headgroup-volume inferred by the negative charge. As pH is lowered oleic acid is increasingly neutralized through protonation, which decreases the effective headgroup-volume and leads to membrane instability.[1]

Dept. of Micro- and Nanotechnology, Technical University of Denmark, DTU Nanotech, Building 345 East, DK-2800 Kgs. Lyngby, Denmark. E-mail: tlan@nanotech.dtu.dk

† Electronic Supplementary Information (ESI) available: Additional supporting experimental results. See DOI: 10.1039/c1sm05818e/

The fusogenic abilities of large unilamellar vesicles (LUVs) have previously been studied using fluorescence spectroscopy, by monitoring Förster Resonance Energy Transfer (FRET) of a donor–acceptor pair attached to lipids in the fusogenic liposomal membrane.[5–7] Fusion with an unlabeled liposome results in dual fluorescent probe dilution, leading to decreased FRET. The efficiency of FRET decreases with the sixth power of the donor–acceptor separation,[8] making it highly sensitive to probe dilution. In addition to the extensive use of FRET in fluorescence spectroscopy fusion studies, it has been employed in fluorescence microscopy to visualize and measure molecular interactions in cells.[9,10]

Mixing of lipids from the fusogenic liposome and the target liposomes could also occur by hemifusion, *i.e.* fusion of the outer membrane only, in which case the aqueous contents of the two liposomes would not be mixed. Several assays for studying mixing of aqueous content during fusion have been reported, most of which employ quenching or dequenching of water-soluble fluorophores.[11–15]

Previous quantitative fusion studies have focused mainly on LUV–LUV self-fusion,[5–7,11] where experiments are performed in bulk solution and results are average values that are not easily interpreted, which has given rise to erroneous conclusions. It is not clear in many studies if the aqueous content transfer or leakage is dominant during liposome fusion. Some qualitative

View Article Online

Published on 11 August 2011. Downloaded by Pennsylvania State University on 05/03/2016 05:08:12.

and semiquantitative investigations of giant unilamellar vesicles (GUVs) fusing with LUVs or with other GUVs have been reported,[16–21] but to the best of our knowledge no previous reports have successfully combined studies of quantitative lipid mixing and content mixing.

GUVs have previously been used extensively for assessing mechanical properties of lipid membranes and interactions of macromolecules with membranes,[22,23] but GUVs are in addition quite advantageous to use in fusion studies,[24] mainly due to their size which provides several benefits. Firstly, they can be observed in an optical microscope and can be characterized *in situ* during fusion studies with respect to size and lamellarity, both of which are important factors in membrane fusion. In studies with LUVs, the hydrodynamic radius can be found using dynamic light scattering (DLS) and the lamellarity and size can be found using cryogenic transmission electron microscopy (Cryo-TEM), but typically not under fusion conditions. Secondly, the size and curvature of GUVs is similar to cells, which is an advantage when studying fusogenic liposomes designed to fuse with the plasma membrane, as evidence suggests that fusion is affected by membrane curvature.[25,26]

Here we quantify pH-dependent fusion between fusogenic LUVs and stable GUVs by confocal fluorescence microscopy, using a combination of a modified version of the FRET lipid mixing assay and a modified version of a contents mixing assay based on fluorescence dequenching. Both assays are outlined in Fig. 1. The FRET donor used here is the fluorophore lipid DOPE-N-(7-nitro-2–1,3-benzoxadiazol-4-yl) (NBD-DOPE) and the FRET acceptor is DOPE-N-(lissamine rhodamine B sulfonyl) (Rho-DOPE). Fusogenic LUVs composed of oleic acid (OA) and DOPE in different ratios have previously been described[1,27,28] and here we use OA:DOPE in the molar ratio 4 : 6.

Calcein was encapsulated in LUVs at a self-quenching concentration to limit background signal from LUVs and to ensure a large signal in GUVs despite the large dilution. Furthermore, leakage of calcein during fusion will lead to an increase in background signal, which can be used to monitor the efficiency with which the aqueous content is transferred from LUVs to GUVs.

Experimental

Materials

All lipids, fluorophore lipids and cholesterol were purchased from Avanti Polar Lipids (USA) and were used without further purification. Calcein, glucose, sucrose, glycine, MES and other chemicals were purchased from Sigma–Aldrich (Denmark).

Liposome preparation and characterization

GUVs. GUVs were prepared by electroformation[29] using a custom-built chamber.[30] Lipids were dissolved in $CHCl_3$:MeOH (9 : 1 v/v) at 0.4 mM and a few droplets of 1–2 μL were deposited on two parallel platinum electrodes, to a total amount of 5 μL. The organic solvent was evaporated and the electrodes were placed under vacuum overnight to remove remaining solvent. The electrodes were subsequently submersed in 150 μL electroformation buffer (100 mM sucrose and either 5 mM glycine or 20 mM MES, 100 mOsmol) adjusted to the desired pH. GUVs were grown at room temperature for 3 h under an AC voltage of 1 V (gradually increased from 100 mV during the first

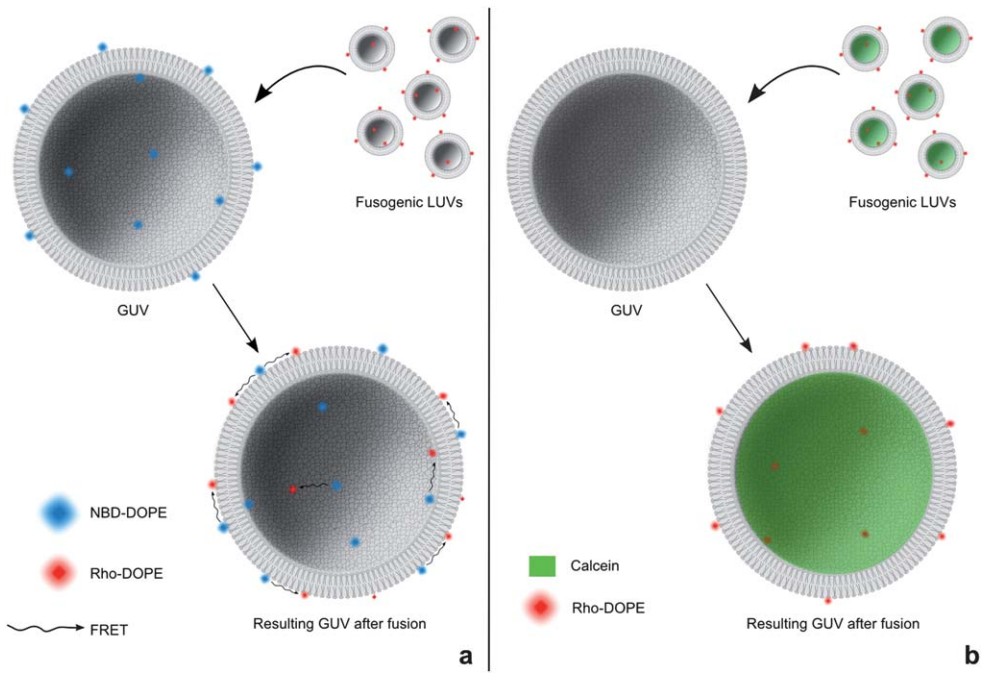

Fig. 1 Schematic illustration of the fusion assays. a) Lipid mixing assay. Fusion of rhodamine-labeled fusogenic LUVs with NBD-labeled GUVs will lead to FRET transfer from NBD to rhodamine. b) Contents mixing assay. Fusion of rhodamine-labeled LUVs containing calcein with empty GUVs will lead to a rhodamine-signal in the GUV membrane and a calcein-signal in the GUV lumen. Not drawn to scale.

 This journal is © The Royal Society of Chemistry 2011

View Article Online

Published on 11 August 2011. Downloaded by Pennsylvania State University on 05/03/2016 05:08:12.

hour) at 10 Hz, after which the GUVs were detached by decreasing the frequency to 4 Hz for 30 min. The AC generator used was a FG 100 Function Generator from Digimess.

Positive GUVs were composed of palmitoyloleoylglycerophosphocholine (POPC), cholesterol (Chol, 40 mol%), dioleoyltrimethylammoniumpropane (DOTAP, 5 or 10 mol%) and NBD-DOPE (1 mol%).

Negative GUVs were composed of POPC (49 mol%), Chol (40 mol%), palmitoyloleoylglycerophosphoglycerol (POPG, 10 mol%) and NBD-DOPE (1 mol%)

LUVs. 5 mM of lipids were dissolved in $CHCl_3$:MeOH (9 : 1 v/v). Solvent was evaporated under N_2-flow and placed under a vacuum overnight. The lipid film was rehydrated to 5 mM in glycine buffer (5 mM glycine, 50 mM NaCl, 1 mM EDTA, 100 mOsmol) at pH 9.5. The solution was vortexed frequently for 1 h and subjected to 5 cycles of freeze–thawing (isopropanol/dry-ice and 40 °C water bath). The solution was extruded by passing it 21 times through a 100 nm polycarbonate filter in an Avanti extruder. The composition of fusogenic LUVs was OA:DOPE (40 : 60 mol/mol) with 1 mol% Rho-DOPE.

LUVs with encapsulated calcein. As above, with lipids dissolved at 25 mM, using a glycine buffer containing 25 mM calcein and 10 freeze–thaw cycles. After extrusion the liposomes were separated from free calcein on a Sephadex G-50 column, using glycine buffer as eluent.

Final calcein concentration in the liposomes was measured by disrupting the LUVs with 0.1 vol% Triton X-100 and measuring the resulting signal using the confocal microscope, along with a standard curve for calcein (see ESI, Table 1†). Combined with the final lipid concentration found from phosphorous analysis (described below) and the size of the liposomes found by DLS (described below) we could estimate the concentration of calcein in the liposomes. This was performed in triplicates for two different concentrations of liposomes in the microscope chamber. Furthermore, it was checked whether triton affected calcein fluorescence, which was not the case.

Dynamic light scattering (DLS) measurements. A ZetaPALS Zeta Potential Analyzer (Brookhaven Instruments Corporation, USA) was used to determine vesicle size after extrusion. In all experiments a hydrodynamic diameter of approx. 130 nm was found for all LUVs.

Phosphorous analysis. Lipid concentration in liposome suspensions after extrusion (and column purification) was measured by phosphorous analysis, as previously described.[31] For LUVs with an initial concentration of 5 mM, a typical final concentration after extrusion was 3.6 mM. For LUVs with an initial concentration of 25 mM, a typical final concentration after extrusion and column purification was 2.6 mM. All measurements were performed in triplicates.

Confocal fluorescence microscopy

A Leica TCS SP5 AOBS confocal microscope (Leica Microsystems, Germany) with a 100× oil objective (NA 1.4) was used to image GUVs.

In fluorescence imaging, NBD was excited at 458 nm and the emission was measured in the 470–550 nm range. Rhodamine B was excited at 561 nm and the emission was measured in the range of 600–700 nm (not measured at emission maximum to limit bleed-through from NBD emission). Calcein was excited at 496 nm and the emission was measured in the range of 510–550 nm. The laser power was kept at a minimum to allow a sufficient signal, while avoiding bleaching.

The GUV suspension in the sucrose buffer was diluted at 1 : 1 with a glucose buffer (100 mM glucose and either 20 mM glycine or 20 mM MES, 100 mOsmol) before imaging. The glucose buffer was used to adjust pH and to ease imaging by making the GUVs settle on the bottom due to density differences in the buffers. For fusion experiments, the GUVs in sucrose/glucose were mixed with the fusogenic LUV suspension 4 : 1 (v/v) and was left for 30 min before imaging.

Quantification program

A program for quantification of fluorescence signal in GUV membranes was written in Python. The program input was a microscopy image of a single GUV, exported as a Tiff-file using Leica microscope software. The GUV membrane was approximated by a circular band with a defined width and was found by an initial guess for the center and radius followed by an implementation of the Nelder–Mead Simplex algorithm from the SciPy optimization library.[32] The initial guess for the GUV center was found by averaging over all pixel positions weighed by intensity and the guess for the radius was found by averaging over the radial distance to the pixels weighed by intensity. In both cases a cut-off was used to limit the influence of background noise.

At present, this program is only able to find a membrane when there is a single GUV in the image and the background signal is low. Therefore it cannot be used to measure the rhodamine signal in a GUV membrane when rhodamine is excited, due to the large background signal from the surrounding LUVs, so in that case it was performed manually, using Leica software.

Results and discussion

We studied fusogenic LUVs composed of OA and DOPE in a 4 : 6 ratio, in which composition the apparent pK_a (pK_a^{app}) of OA is 6.5 (found by titration of the liposomes, data not shown), consistent with previous investigations of the acidity constant of oleic acid in lipid bilayers.[33,34] We hypothesize that the instability in the LUV membrane will cause it to fuse with an adjacent, stable GUV membrane at pH 6.1. Furthermore, we hypothesize that electrostatic attraction between the fusogenic liposome and the target GUV is important for the degree of fusion. Using the Henderson–Hasselbalch equation and the pK_a^{app}-value of OA, approximately 27% of OA is deprotonated at pH 6.1, thus the liposome contains approximately 11 mol% of negatively charged lipids at this pH. The Henderson–Hasselbalch equation assumes a complete deprotonation of the acid at high pH-values, which may not be the case for acids in liposomes, as discussed by Lieckfeldt *et al.*[33] Thus, the charge density of the liposome is likely to be lower than expected, but still negative (zeta potential was measured to be −35 mV at pH 7.3).

View Article Online

Published on 11 August 2011. Downloaded by Pennsylvania State University on 05/03/2016 05:08:12.

Due to the negative charge of the fusogenic liposomes, fusion is expected to be limited for GUVs containing negatively charged lipids and increase with increasing density of positively charged lipids in GUVs. At higher pH-values the OA:DOPE liposomes are expected to be stable, which is tested in control experiments at pH 9.5. We ascertained that the GUVs were stable at both pH-values before beginning fusion experiments and we distinguished unilamellar GUVs from multilamellar GUVs by a visual inspection of the fluorescence intensity and the level of membrane undulations, as described by Akashi *et al.*[35]

Lipid mixing assay

Visualization of membrane fusion. When fusogenic LUVs were mixed with GUVs containing a 10 mol% positively charged lipid (DOTAP) in POPC at pH 6.1, we observed rhodamine fluorescence in the GUV membrane, which we interpreted as a result of fusion (Fig. 2). Neither positive GUVs at pH 9.5 nor negative GUVs (containing 10 mol% POPG) resulted in fusion, showing that the fusion is highly dependent on both the pH and the electrostatic attraction between the LUVs and the GUVs. For the positive GUVs at pH 6.1 the rhodamine signal is distributed evenly along the membrane, which indicates that the rhodamine signal is the result of fusion, as opposed to LUVs adhering to the GUV surface. For positive GUVs at both pH-values, a few GUVs exhibited bright spots along the membrane, which could be due to aggregates of LUVs adhering to the GUV membrane.

The ionic strength of the solution/buffer, in which the membrane fusion takes place, is an important parameter governing electrostatic interactions between the fusing membranes due to screening of charges. The Debye screening length, λ_D,[36,37] provides a measure of the distance, d, at which the screening of the electrostatic potentials is moderate ($d = \lambda_D$) and above which it is effective ($d > \lambda_D$). In the present context λ_D should be compared to the interbilayer distance necessary for fusion to occur. In a theoretical evaluation (focusing on hydration repulsion forces between neutral membranes) it has been proposed that this distance is ~1 nm.[38] An estimate of the Debye screening length in low salt ($\lambda_D \approx 3$ nm, 10 mM NaCl, $T = 298$ K, $\varepsilon_r = 78$) predicts that the membrane charges will be of importance for membrane fusion. This prediction is supported by our observation of a lack of fusion between OA:DOPE liposomes and negative GUVs and the effective fusion with positive GUVs at 10 mM NaCl (Fig. 2), as well as the low degree of self-fusion we observe among the fusogenic LUVs. At high salt, a more efficient screening of charges is predicted ($\lambda_D \approx 0.8$ nm, 150 mM NaCl, $T = 298$ K, $\varepsilon_r = 78$). Thus, the attraction between negative fusogenic LUVs and positive GUVs, as well as the repulsion amongst fusogenic LUVs and between fusogenic LUVs and negative GUVs, will be decreased at this salt concentration. In support of these predictions, we actually observe some degree of fusion with negatively charged GUVs at 150 mM NaCl, as well as more pronounced self-fusion between the fusogenic LUVs (data not shown).

Quantification of membrane fusion. To aid quantification, we wrote a simple program that finds the membrane of the GUV in an image and quantifies the fluorescence intensity of the membrane. This ensures that the data-treatment is not biased and allows for larger amounts of data to be analyzed. An example of the program output is shown in Fig. 3 and the program is described further in the Experimental section.

We prepared a series of GUVs labeled with NBD-DOPE and increasing amounts of Rho-DOPE, to construct a standard curve for rhodamine concentration in the GUV membrane (see ESI, Fig. S2†). Fig. 2 shows the fluorescence signal when only NBD is excited, along with the signal when both NBD and rhodamine are excited. In the following quantification we use the ratio between the rhodamine signal and NBD signal when only NBD is excited, *i.e.* the FRET signal. The ratio will increase with

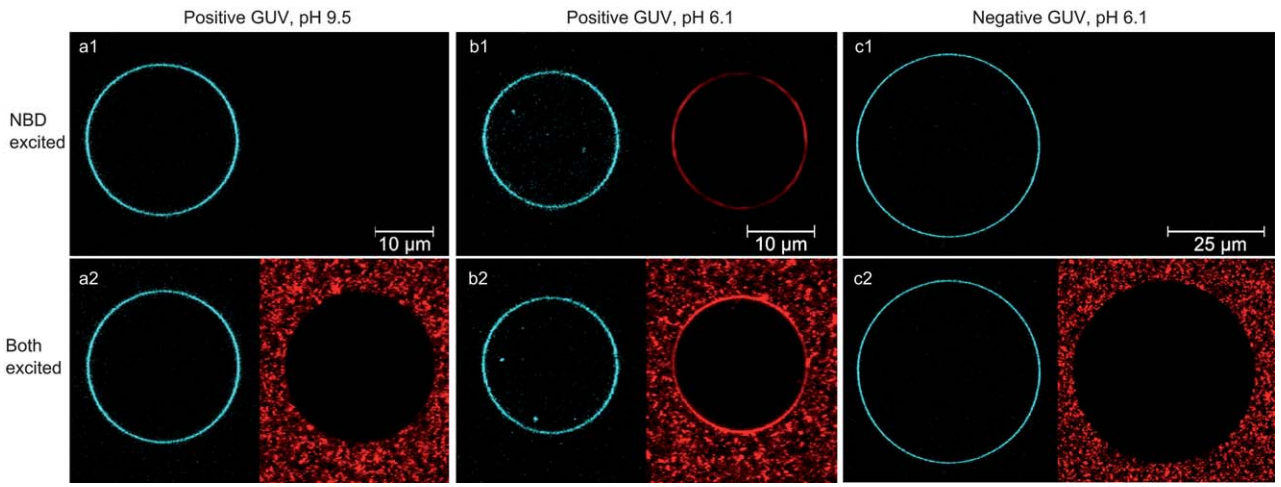

Fig. 2 Confocal microscopy images of GUVs labeled with NBD-DOPE (blue) and fusogenic LUVs labeled with Rho-DOPE (red). In the upper panels only NBD is excited and in the lower panels both NBD and rhodamine are excited. Each collection of four images (*e.g.* a1 and a2) is a single GUV and above each collection is the specified GUV type and pH. At pH 6.1 for a positive GUV (b) there is a clear rhodamine signal in the GUV membrane when both fluorophores are excited (b2) and a FRET-signal when only NBD is excited (b1). Furthermore, the NBD-signal is slightly decreased, consistent with FRET transfer to rhodamine. Neither positive GUVs at pH 9.5 (a), nor negative GUVs at pH 6.1 (c) display this, apart from very small bleed-through signals.

 This journal is © The Royal Society of Chemistry 2011

View Article Online

Published on 11 August 2011. Downloaded by Pennsylvania State University on 05/03/2016 05:08:12.

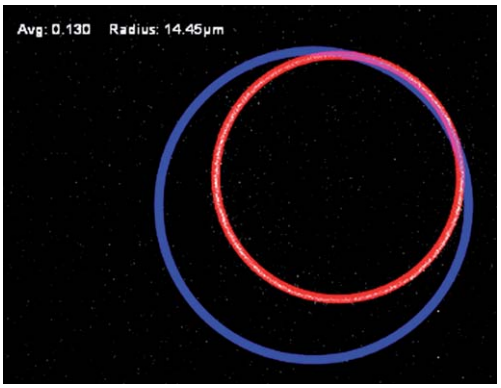

Fig. 3 An example of the GUV program output. The blue ring is the initial guess for the GUV membrane and the red ring is the final position after optimization, in which the intensity is measured. In this image the red ring is a good match for the white signal from the GUV membrane, *i.e.* the program was successful in finding the GUV membrane. The average intensity and the radius of the GUV is shown in the upper left corner, as well as written to a csv-file for data-treatment.

increasing fusion, as the rhodamine signal increases and the NBD signal decreases.

From the standard curve we correlate the fluorescence intensity signal in a GUV membrane with the rhodamine concentration in the membrane. We use this to find the approximate number of fusogenic LUVs, n_{LM}, that have fused with the GUV (see ESI for derivation).

$$n_{LM} \approx \frac{x_{GUV}}{x_{LUV}}\left(\frac{r_{GUV}}{r_{LUV}}\right)^2 \quad (1)$$

where r_{GUV} is the radius of the GUV after fusion, r_{LUV} is the average radius of the fusogenic LUVs, x_{GUV} or x_{LUV} is the mole fraction of Rho-DOPE in the GUV or LUV membrane, respectively, and the subscript in n_{LM} signifies that this value was found using the lipid mixing assay. Eqn (1) assumes that no self-fusion has occurred prior to the GUV–LUV fusion, but as stated earlier self-fusion was very limited at the low salt concentration used here. Fig. 4 shows values of n_{LM} for two different GUV compositions at high and low pH.

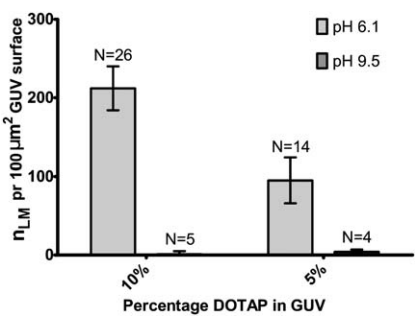

Fig. 4 Number of fusion events by LUVs, n_{LM}, with each GUV per surface area of the GUV. Values are shown for different concentrations of positively charged lipids in the GUVs and for different pH-values. As expected, a higher positive charge leads to an increased amount of fusion events. *N* is the number of GUVs investigated and the error bars are SDOM. For each formulation, data was collected from two independent experiments.

At high pH there is only a negligible signal for both compositions, whereas at low pH n_{LM} is approximately 100 or 200 per 100 μm^2 of GUV surface for 5 and 10 mol% positively charged lipids, respectively. However, for both compositions the deviation in n_{LM} is moderate. This deviation stems from differences in signal within GUVs of the same composition, which appears to be unsystematic. There is no clear relation to size (see ESI, Fig. S1†) or any difference in the GUV appearance. Differences in fusion behavior within a population of liposomes most likely also occurred in previous LUV–LUV fusion studies, but due to averaging it could have gone unnoticed. Here we look at single GUVs, yielding more detailed information about the distribution of fusion events.

A possible explanation for the differences in fusion among GUVs may be an uneven distribution of lipids. There has been a limited investigation of the composition homogeneity of GUVs prepared by electroformation.[39] In Fidorra *et al.*[39] it is argued that GUV composition is fairly homogeneous, based on areas of domains in GUVs from the same preparation. However, these experiments do not include charged lipids. Modified electroformation protocols have been reported,[30,40,41] in which lipids are first reconstituted as LUVs or SUVs before deposition on electrodes for GUV formation (see Experimental section). This modification may decrease the possible lipid heterogeneity in GUVs.

The rhodamine/NBD standard curve is performed only for GUVs with 10 mol% DOTAP and as the fluorescence intensity of NBD and rhodamine is sensitive to the surroundings, the standard curve should only be used for GUVs with a very similar composition. It has been verified spectroscopically that the fluorescence and FRET-efficiency of NBD-DOPE and Rho-DOPE is very similar in POPC:Chol:DOTAP LUVs and OA:DOPE LUVs, which indicates that OA and DOPE entering the GUV membrane during fusion does not compromise the use of standard curves in fusion studies. However, this could be system dependent and should be checked when conducting fusion studies using other membrane lipid compositions.

In previous LUV–LUV fusion assays, the bulk ratio between fusogenic liposomes and target liposomes is an important factor,[7] which affects the measured extent of fusion. In such fusion experiments the liposomes are typically present at approximately equal amounts, or there is an excess of target liposomes.[7] However, in the present work, the liposome ratio can not be used in the same manner, due to the large size difference of LUVs and GUVs.

While calculating n_{LM}, we find that the resulting GUV after fusion contains a large amount of lipids from fusogenic liposomes. For GUVs with 10 mol% of positively charged lipids, up to half of the resulting GUV lipids are from fusogenic liposomes, and for GUVs with 5 mol% positively charged lipids it is up to a third of the resulting GUV lipids. This corresponds well with the electrostatic dependence of fusion, as fusion seems to continue until the GUV charge has been neutralized by the negatively charged lipids in the fusogenic liposomes.

Contents mixing assay

Visualization of contents mixing during fusion. When fusogenic LUVs containing calcein were mixed with GUVs containing

View Article Online

Published on 11 August 2011. Downloaded by Pennsylvania State University on 05/03/2016 05:08:12.

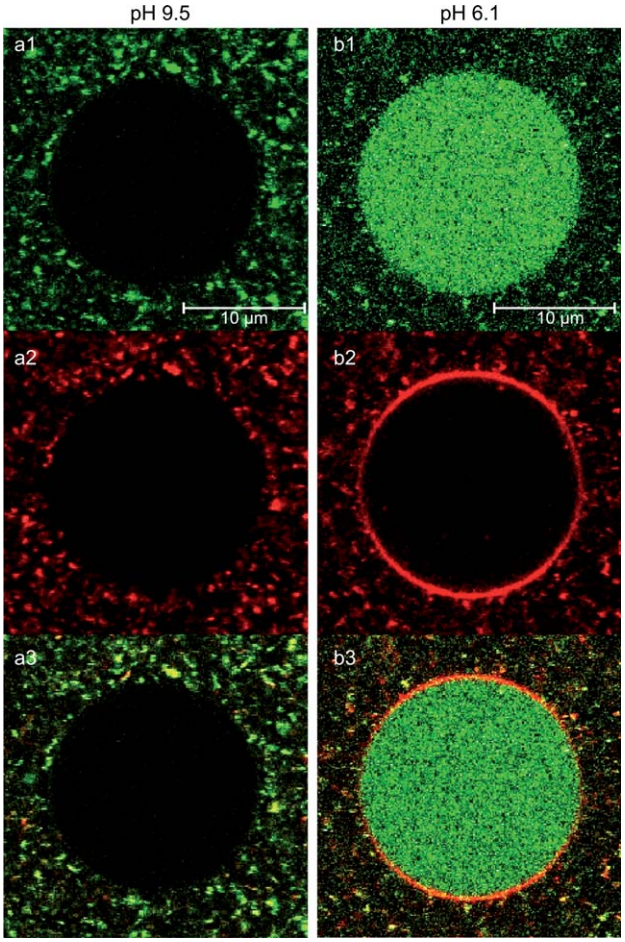

Fig. 5 Confocal microscopy images of positive GUVs and fusogenic LUVs. The LUVs are labeled with Rho-DOPE (red) in the membrane and contain encapsulated calcein (green) in the aqueous lumen. In all images both fluorophores are excited and images labeled 1, 2 and 3 show the calcein signal, the rhodamine signal and overlays of the two signals, respectively. At pH 6.1 (b) there is a clear calcein signal in the lumen of the GUV and a rhodamine signal in the GUV membrane, consistent with membrane fusion and transfer of aqueous content from the LUVs to the GUV. At pH 9.5 (a) there is no signal neither in the membrane nor lumen.

10 mol% DOTAP at pH 6.1 (Fig. 5), we observed a distinct calcein signal in the GUV lumen, whereas at pH 9.5 there was no signal. Fusion was further confirmed by the transfer of Rho-DOPE from the LUVs to the GUV membrane.

Leakage of encapsulated calcein during fusion would lead to an increased background signal at a low pH, which was not observed. This indicates that either all calcein is transferred during fusion, or the leaked amount is too small to be detected. When LUVs were disrupted with triton, the calcein intensity increased significantly (see ESI, Fig. S4†). This shows that complete leakage of encapsulated calcein during fusion would lead to a measurable increase in background signal. Furthermore, leakage of calcein during LUV–LUV self-fusion events would lead to an increase in the background signal, which was not due to the leakage during LUV–GUV fusion. However, experiments suggest that the self-fusion occurs without substantial leakage (see ESI, Fig. S4†).

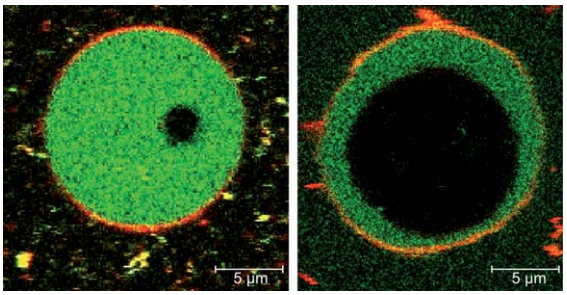

Fig. 6 Confocal microscopy images of positive GUVs and fusogenic LUVs at pH 6.1. The LUVs are labeled with Rho-DOPE (red) in the membrane and contain encapsulated calcein (green) in the aqueous lumen. In both images both fluorophores are excited. The GUVs in the images have isolated vesicles within them and calcein is only transferred to the outer lumen, which shows that calcein does not cross the lipid membrane on the time scale of the experiment. The lack of rhodamine signal in the inner membrane also shows that the fluorophore lipids are not transferred to neighboring membranes within the time frame of the experiment.

Behavior of fluorophore labels in GUVs. Some GUVs contained smaller vesicles, wherein no calcein or rhodamine signal was evident after fusion (Fig. 6). This shows that calcein cannot cross the GUV membrane and Rho-DOPE is not transferred to neighboring membranes within the time frame of the experiment, indicating that both labels only enter GUVs during fusion events. The ability to track fluorophore labels while they interact with the GUV membrane, is a distinct advantage of this assay over conventional spectroscopic assays.

Quantification of contents mixing during fusion. The calcein signal in the GUVs was correlated to calcein concentration by a standard curve (see ESI, Fig. S2†), where we verified that the quantum yield of calcein did not change significantly between the two pH-values used. The final concentration of calcein in the fusogenic LUVs found by triton disruption (see experimental) was 13 ± 0.2 mM. If we assume that all calcein is transferred to the GUV during fusion, the number of fusion events with a single GUV, n_{CM}, is given by

$$n_{CM} \approx \frac{c_{GUV}}{c_{LUV}}\left(\frac{r_{GUV}}{r_{LUV}}\right)^3 \quad (2)$$

where c_{GUV} is the calcein concentration in a GUV, c_{LUV} is the calcein concentration in the LUVs, r_{GUV} is the radius of the GUV after fusion, r_{LUV} is the average radius of the fusogenic LUVs and the subscript in n_{CM} signifies that this value was found using the contents mixing assay.

n_{CM} can be compared to n_{LM} to estimate how efficiently the aqueous content is transferred during fusion and for GUVs containing 10 mol% DOTAP (Fig. 7), it appears to be transferred without a large extent of leakage.

In the employed experimental setup the two assays are performed in separate experiments, due to the large overlap of NBD and calcein excitation and emission. However, by using another combination of fluorophores, these two assays could be combined. In our case, to verify that the extent of fusion was the same in the two assays, we measured the rhodamine signal in the

 This journal is © The Royal Society of Chemistry 2011

View Article Online

Published on 11 August 2011. Downloaded by Pennsylvania State University on 05/03/2016 05:08:12.

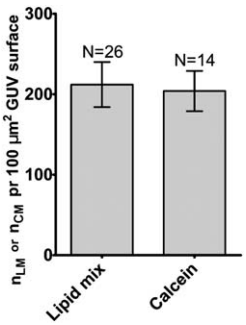

Fig. 7 Number of fusogenic LUVs fusing with each GUV per surface area of the GUV, found using the lipid mixing assay (n_{LM}) and calcein transfer assay (n_{CM}). Both results are for GUVs with 10 mol% DOTAP and should be equal if calcein is transferred without leakage during fusion. *N* is the number of GUVs investigated and error bars are SDOM. For each assay, data was collected from two independent experiments.

GUV membrane after fusion (when only rhodamine was excited) which should be the same in the two cases. We found very similar values.

In these experiments the high degree of fusion ensures a high calcein signal in the GUV lumen, but the large dilution of calcein when entering the GUV membrane could limit the sensitivity for less efficient fusion events. Other volume transfer assays employ enzymatic cleavage of a non-fluorescent substrate to a fluorescent product,[19] which is not affected to the same degree by dilution.

Conclusion

The quantitative fusion assay presented in this article is distinguished from previously reported fusion assays in the ability to quantify number of fusion events combined with how efficiently the contents of fusogenic liposomes is transferred during fusion. This is very useful, *e.g.* in drug delivery related studies, as the amount of drug delivered to a cell obviously is important. In addition, this assay is advantageous compared to conventional spectroscopic fusion assays as it has less averaging effects, *in situ* characterization of GUVs and gives a better understanding of the behavior of fluorescent probes during fusion experiments.

Here, GUVs are used as simple model systems for cells in order to quantify membrane fusion alone, at easily controllable conditions, which is far more complicated to do in studies with cells. In future studies the composition of GUVs can be changed to increase biological relevance and resemblance to cells, or it can be replaced by ghost-cells. The lipid mixing part of the assay can not be used directly for fusion with cells, as the cell membrane can not be labeled with fluorophore lipids, but the assay is easily adjusted for this purpose.

The fusion assay is only demonstrated for pH-dependent fusion in this article, but it is not restricted to this type of fusion and can be used for other systems, such as fusion induced by ions,[15,42] enzymes[43] or heat.[44]

In the experiments presented here, the lipid mixing assay and the content mixing assay are performed separately, due to the close proximity of NBD and calcein excitation/emission, but in principle it could be adjusted to allow simultaneous measurements by choosing a different set of fluorophores.

Acknowledgements

We gratefully acknowledge the Technical University of Denmark and the Danish Council for Strategic Research, NABIIT, grant no. 2106-07-0033 and 2106-08-0081 for supporting this work.

References

1 D. C. Drummond, M. Zignani and J. Leroux, *Prog. Lipid Res.*, 2000, **39**, 409–460.
2 S. Simões, J. N. Moreira, C. Fonseca, N. Düzgünes and M. C. P. de Lima, *Adv. Drug Delivery Rev.*, 2004, **56**, 947–965.
3 J. Connor and L. Huang, *Cancer Res.*, 1986, **46**, 3431–3435.
4 T. L. Andresen, S. S. Jensen and K. Jørgensen, *Prog. Lipid Res.*, 2005, **44**, 68–97.
5 J. Connor, M. B. Yatvin and L. Huang, *Proc. Natl. Acad. Sci. U. S. A.*, 1984, **81**, 1715–1718.
6 D. K. Struck, D. Hoekstra and R. E. Pagano, *Biochemistry*, 1981, **20**, 4093–4099.
7 A. L. Bailey and P. R. Cullis, *Biochemistry*, 1997, **36**, 1628–1634.
8 J. R. Lakowicz, *Principles of Fluorescence Spectroscopy*, Springer, 3rd edn, 2006.
9 A. Periasamy, R. N. Day, K. F. Sullivan and S. A. Kay, *Green Fluorescent Proteins*, Academic Press, 1998, vol. 58, pp. 293–314.
10 R. B. Sekar and A. Periasamy, *J. Cell Biol.*, 2003, **160**, 629–633.
11 H. Ellens, J. Bentz and F. C. Szoka, *Biochemistry*, 1985, **24**, 3099–3106.
12 R. A. Blackwood, J. E. Smolen, R. J. Hessler, D. M. Harsh and A. Transue, *Biochem. J.*, 1996, **314**, 469–475.
13 J. Connor and L. Huang, *J. Cell Biol.*, 1985, **101**, 582–589.
14 J. Rosenberg, N. Düzgünes and Ç. Kayalar, *Biochim. Biophys. Acta, Biomembr.*, 1983, **735**, 173–180.
15 J. Wilschut, N. Düzgünes, R. Fraley and D. Papahadjopoulos, *Biochemistry*, 1980, **19**, 6011–6021.
16 G. Lei and R. C. MacDonald, *J. Membr. Biol.*, 2008, **221**, 97–106.
17 T. Tanaka and M. Yamazaki, *Langmuir*, 2004, **20**, 5160–5164.
18 V. Marchi-Artzner, T. Gulik-Krzywicki, M. Guedeau-Boudeville, C. Gosse, J. Sanderson, J. Dedieu and J. Lehn, *ChemPhysChem*, 2001, **2**, 367–376.
19 N. Kahya, E. Pécheur, W. P. de Boeij, D. A. Wiersma and D. Hoekstra, *Biophys. J.*, 2001, **81**, 1464–1474.
20 D. Tareste, J. Shen, T. J. Melia and J. E. Rothman, *Proc. Natl. Acad. Sci. U. S. A.*, 2008, **105**, 2380–2385.
21 F. M. Menger and K. Gabrielson, *J. Am. Chem. Soc.*, 1994, **116**, 1567–1568.
22 P. Méléard, C. Gerbeaud, P. Bardusco, N. Jeandaine, M. D. Mitov and L. Fernandez-Puente, *Biochimie*, 1998, **80**, 401–413.
23 J. Henriksen, A. C. Rowat and J. H. Ipsen, *Eur. Biophys. J.*, 2004, **33**, 732–741.
24 P. L. Luisi and P. Walde, *Giant Vesicles: Perspectives in Supramolecular Chemistry*, Wiley-Interscience, 1st edn, 2000.
25 S. Nir, J. Wilschut and J. Bentz, *Biochim. Biophys. Acta, Biomembr.*, 1982, **688**, 275–278.
26 B. R. Lentz, G. F. McIntyre, D. J. Parks, J. C. Yates and D. Massenburg, *Biochemistry*, 1992, **31**, 2643–2653.
27 R. M. Straubinger, N. Düzgünes and D. Papahadjopoulos, *FEBS Lett.*, 1985, **179**, 148–154.
28 N. Düzgünes, R. M. Straubinger, P. A. Baldwin, D. S. Friend and D. Papahadjopoulos, *Biochemistry*, 1985, **24**, 3091–3098.
29 M. Angelova, S. Soléau, P. Méléard, F. Faucon and P. Bothorel, *Trends in Colloid and Interface Science VI*, Springer Berlin/Heidelberg, 1992, vol. 89, pp. 127–131.
30 P. Méléard, L. A. Bagatolli, T. Pott and N. Düzgünes, *Giant Unilamellar Vesicle Electroformation*, Academic Press, 2009, vol. 465, pp. 161–176.
31 K. Itaya and M. Ui, *Clin. Chim. Acta*, 1966, **14**, 361–366.
32 E. Jones, T. Oliphant and P. Peterson, *SciPy: Open source scientific tools for Python*, 2001.
33 R. Lieckfeldt, J. Villalaín, J. C. Gómez-Fernández and G. Lee, *Pharm. Res.*, 1995, **12**, 1614–1617.
34 S. Salentinig, L. Sagalowicz and O. Glatter, *Langmuir*, 2010, **26**, 11670–11679.

View Article Online

Published on 11 August 2011. Downloaded by Pennsylvania State University on 05/03/2016 05:08:12.

35 K. Akashi, H. Miyata, H. Itoh and K. Kinosita, *Biophys. J.*, 1996, **71**, 3242–3250.
36 J. N. Israelachvili, in *Intermolecular and Surface Forces*, Academic Press, 2nd edn, 1992, ch. 12, pp. 213–256.
37 N. J. Zuidam and Y. Barenholz, *Biochim. Biophys. Acta, Biomembr.*, 1997, **1329**, 211–222.
38 Y. Kozlovsky, A. Efrat, D. A. Siegel and M. M. Kozlov, *Biophys. J.*, 2004, **87**, 2508–2521.
39 M. Fidorra, A. Garcia, J. H. Ipsen, S. Härtel and L. A. Bagatolli, *Biochim. Biophys. Acta, Biomembr.*, 2009, **1788**, 2142–2149.
40 T. Pott, H. Bouvrais and P. Méléard, *Chem. Phys. Acta*, 2008, **154**, 115–119.
41 P. Girard, J. Pcraux, G. Lenoir, P. Falson, J. Rigaud and P. Bassereau, *Biophys. J.*, 2004, **87**, 419–429.
42 D. Papahadjopoulos, W. J. Vail, W. A. Pangborn and G. Poste, *Biochim. Biophys. Acta, Biomembr.*, 1976, **448**, 265–283.
43 T. L. Andresen, D. H. Thompson and T. Kaasgaard, *Mol. Membr. Biol.*, 2010, **27**, 353–363.
44 R. W. H. Ruigrok, S. R. Martin, S. A. Wharton, J. J. Skehel, P. M. Bayley and D. C. Wiley, *Virology*, 1986, **155**, 484–497.

 This journal is © The Royal Society of Chemistry 2011